Are There Sterile Neutrinos at the eV Scale?

Joachim Kopp,[1] Michele Maltoni,[2] and Thomas Schwetz[3]

[1]*Fermilab, Theoretical Physics Department, P.O. Box 500, Batavia, Illinois 60510, USA*
[2]*Instituto de Física Teórica UAM/CSIC, Calle de Nicolás Cabrera 13-15, E-28049 Madrid, Spain*
[3]*Max-Planck-Institut für Kernphysik, P.O. Box 103980, 69029 Heidelberg, Germany*

(Received 31 March 2011; published 23 August 2011)

New predictions for the antineutrino flux from nuclear reactors suggest that reactor experiments may have measured a deficit in this flux, which can be interpreted in terms of oscillations between the known active neutrinos and new sterile states. We perform a reanalysis of global short-baseline neutrino oscillation data in a framework with one or two sterile neutrinos. While one sterile neutrino is still not sufficient to reconcile the signals suggested by reactor experiments and by the LSND and MiniBooNE experiments with null results from other searches, we find that, with the new reactor flux prediction, the global fit improves considerably when two sterile neutrinos are introduced.

DOI: 10.1103/PhysRevLett.107.091801 PACS numbers: 14.60.St, 14.60.Pq

Introduction.—By now a standard paradigm of neutrino physics has emerged. A beautiful series of experiments has established the phenomenon of neutrino oscillations. Results from solar, atmospheric, reactor, and accelerator neutrino experiments can be accommodated nicely by oscillations of the three neutrinos of the standard model, the so-called ''active'' neutrinos, with mass-squared differences of order 10^{-4} and 10^{-3} eV^2, see [1,2] for recent fits and references. There are, however, a few experimental results which cannot be explained within this framework and seem to require additional neutrinos with masses at the eV scale [3,4]. Such neutrinos cannot participate in the weak interactions due to collider constraints, and are therefore called ''sterile'' neutrinos.

Recently, another hint for sterile neutrinos has emerged from a reevaluation of the expected electron antineutrino ($\bar{\nu}_e$) flux emitted by nuclear reactors [5]. The new prediction is $\sim$3% higher than what was previously assumed [6]. If confirmed, this result would imply that all existing neutrino oscillation searches at nuclear reactors have observed a deficit of $\bar{\nu}_e$, which can be interpreted in terms of oscillations at baselines of order 10–100 m [7]. At typical reactor antineutrino energies of few MeV, standard oscillations of the three active neutrinos require baselines of a least 1 km. Hence, the ''reactor anomaly'' can only be accommodated if at least one sterile neutrino with mass at the eV scale or higher is introduced. This is particularly intriguing because also the long-standing ''LSND anomaly'' [3], as well as the more recent MiniBooNE antineutrino results [4] suggest the existence of a sterile neutrino in that mass range.

Previous phenomenological studies [8–10] have been performed in a framework in which the standard three-active neutrino scenario is amended by adding one (''3 + 1'') or two (''3 + 2'') sterile neutrinos with masses at the eV scale. These studies came to the conclusion that an explanation of the aforementioned anomalies within these sterile neutrino scenarios is in conflict with various constraints from other neutrino oscillation searches at short baselines (SBL), including also data from reactor experiments. In this note we revisit 3 + 1 and 3 + 2 sterile neutrino oscillation schemes in the light of the new reactor neutrino fluxes. We argue that one sterile neutrino is still not sufficient to describe all data, whereas a 3 + 2 framework is now in much better agreement with the data.

Fit of SBL reactors.—Let us first discuss the implications of the new reactor antineutrino flux prediction for reactor data alone by analyzing a set of SBL reactor experiments at baselines $L \lesssim 100$ m [7]. We include full spectral data from the Bugey3 experiment [11] at 15, 40, and 95 m and take into account the Bugey4 [12], ROVNO [13], Krasnoyarsk [14], ILL [15], and Gösgen [16] experiments via the rate measurements summarized in Table II of [7]. Furthermore, we include the Chooz [17] and Palo Verde [18] experiments at $L \simeq 1$ km. We use the neutrino fluxes from the isotopes ^{235}U, ^{239}Pu, ^{238}U, ^{241}Pu obtained in [5] and we include the uncertainty on the integrated flux for each isotope given in Table I of [7], correlated between all experiments. For further technical details see [1].

We perform a fit to these data within the 3 + 1 and 3 + 2 sterile neutrino frameworks, where neutrino oscillations for SBL reactor experiments depend on 2 and 4 parameters, respectively. The parameters are the mass-squared differences Δm^2_{41} and Δm^2_{51} between the eV-scale sterile neutrinos and the light neutrinos, and the elements $|U_{e4}|$ and $|U_{e5}|$ of the leptonic mixing matrix, which describe the mixing of the electron neutrino flavor with the heavy neutrino mass states ν_4 and ν_5. Obviously, for the 3 + 1 case, only ν_4 is present. The best-fit points for the two scenarios are summarized in Table I. To illustrate the impact of sterile neutrinos on the fit to reactor antineutrino data graphically, we compare in Fig. 1 the data to the predictions for the no oscillation case (green dot-dashed) and the best-fit 3 + 1 (blue dashed) and 3 + 2 (red solid)

TABLE I. Best-fit points for the 3 + 1 and 3 + 2 scenarios from reactor antineutrino data. The total number of data points is 69 (Bugey3 spectra plus 9 SBL rate measurements; we have omitted data from Chooz and Palo Verde, which are not very sensitive to the model parameters, but would dilute the χ^2 by introducing 15 additional data points). For no oscillations we have $\chi^2/\text{d.o.f.} = 59.0/69$.

	Δm^2_{41} [eV^2]	$\lvert U_{e4}\rvert$	Δm^2_{51} [eV^2]	$\lvert U_{e5}\rvert$	χ^2/d.o.f.
3 + 1	1.78	0.151			50.1/67
3 + 2	0.46	0.108	0.89	0.124	46.5/65

models. Note that, even for no oscillations, the prediction may deviate from 1 due to nuisance parameters included in the fit to parametrize systematic uncertainties. The fit is dominated by Bugey3 spectral data at 15 and 40 m and the precise rate measurement from Bugey4.

In the lower part of Fig. 2 we show the χ^2 of the SBL reactor fit as a function of Δm^2_{41}. Using the new flux predictions (solid curves) we find a clear preference for sterile neutrino oscillations: the $\Delta\chi^2$ between the no oscillation hypothesis and the 3 + 1 best-fit point is 8.5, which implies that the no oscillation case is disfavored at about 98.6% C.L. (2 d.o.f.). In the 3 + 2 case the no oscillation hypothesis is disfavored compared to the 3 + 2 best-fit point with $\Delta\chi^2 = 12.1$, or 98.3% C.L. (4 d.o.f.). In contrast, with previous flux predictions (dashed curves) the improvement of the fit is not significant, with a $\Delta\chi^2$ between the best-fit points and the no oscillation case of only 3.6 and 4.4 for the 3 + 1 and 3 + 2 hypotheses, respectively.

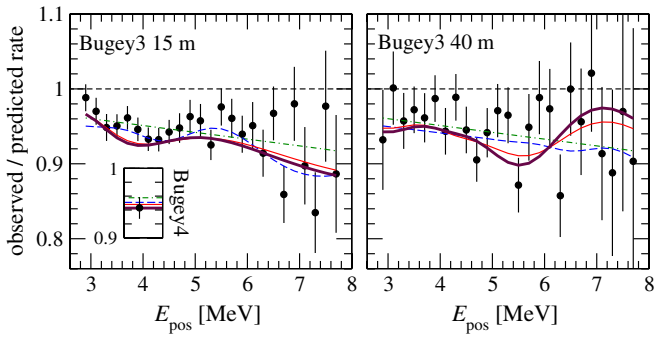

FIG. 1 (color online). Comparison of sterile neutrino models to reactor data: energy spectra from Bugey3 and the rate measurement of Bugey4 (inset). The data points show the ratio of the observed and predicted event numbers where the prediction is based on the new reactor antineutrino fluxes [5] and does not include oscillations. Bugey3 error bars are statistical only, whereas the error on the Bugey4 rate is dominated by systematics. The green dot-dashed curve shows the prediction for the no oscillation hypothesis, the blue dashed and thin light red solid curves correspond to the 3 + 1 and 3 + 2 best-fit points for SBL reactor data (Table I), and the thick dark red solid curve corresponds to the 3 + 2 best-fit point of global SBL data (Table II).

Global analysis of SBL data.—The constraints from the reactor experiments under discussion play an important role in a combined analysis of all SBL oscillation data, including the LSND and MiniBooNE anomalies. LSND has provided evidence for $\bar{\nu}_\mu \to \bar{\nu}_e$ transitions [3], and MiniBooNE has reported an excess of events in the same channel, consistent with the LSND signal [4]. This hint for oscillations is, however, not confirmed by a MiniBooNE search in the $\nu_\mu \to \nu_e$ channel [19], where the data in the energy range sensitive to oscillations is consistent with the background expectation. These results seem to suggest an explanation involving *CP* violation in order to reconcile different results for neutrino and antineutrino searches. An explanation of the LSND and MiniBooNE anomalies via sterile neutrino oscillations requires the mixing matrix elements $\lvert U_{e4}\rvert$ and/or $\lvert U_{e5}\rvert$ to be nonzero. Reactor experiments are sensitive to these parameters, and while analyses using previous flux predictions lead to tight constraints on them, the new fluxes imply nonzero best-fit values (Table I) and closed allowed regions at 98% C.L. Hence, the interesting question arises whether a consistent description of the global data on SBL oscillations (including LSND/MiniBooNE) becomes now possible. To answer this question we perform a fit by including, in addition to the reactor searches for $\bar{\nu}_e$ disappearance, the LSND [3] and MiniBooNE [4,19] results, as well as additional constraints from appearance experiments [20,21], ν_μ disappearance searches [22], and atmospheric neutrinos. Technical details of our analysis can be found in [8,10], and references therein.

In the 3 + 1 scheme the SBL experiments depend on the three parameters Δm^2_{41}, $\lvert U_{e4}\rvert$, and $\lvert U_{\mu 4}\rvert$. Since only one mass scale is relevant in this case it is not possible to obtain

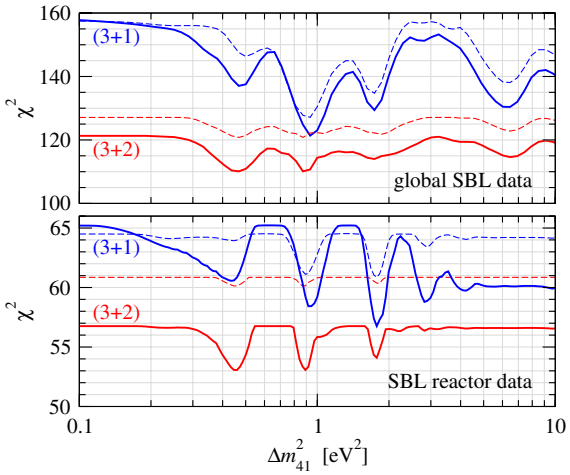

FIG. 2 (color online). χ^2 from global SBL data (upper panel) and from SBL reactor data alone (lower panel) for the 3 + 1 (blue) and 3 + 2 (red) scenarios. Dashed (solid) curves were computed using the old [6] (new [5]) reactor $\bar{\nu}_e$ flux prediction. All undisplayed parameters are minimized over. The total number of data points is 137 (84) for the global (reactor) analysis.

CP violation. Therefore, oscillations involving one sterile neutrino are not capable of reconciling the different results for neutrino (MiniBooNE) and antineutrino (LSND and MiniBooNE) appearance searches. Figure 3 compares the allowed regions from LSND and MiniBooNE antineutrino data to the constraints from the other experiments in the 3 + 1 model. Note that, even though reactor analyses using the new flux prediction prefer nonzero U_{e4}, no closed regions appear for the disappearance bound (solid curve), since $\sin^2 2\theta_{\mathrm{SBL}} = 4|U_{e4}|^2|U_{\mu 4}|^2$ can still become zero if $U_{\mu 4} = 0$. We find that the parameter region favored by LSND and MiniBooNE antineutrino data is ruled out by other experiments, except for a tiny overlap of the three 99% C.L. contours around $\Delta m^2_{41} \approx 1$ eV^2. Note that in this region the constraint from disappearance data does not change significantly due to the new reactor flux predictions. Using the parameter goodness of fit (PG) test from [23] we find a compatibility of the LSND + MiniBooNE ($\bar{\nu}$) signal with the rest of the data only of about 10^{-5}, with $\chi^2_{\mathrm{PG}} = 21.5(24.2)$ for new (old) reactor fluxes. Hence we conclude that the 3 + 1 scenario does not provide a satisfactory description of the data despite the new hint coming from reactors.

Let us move now to the 3 + 2 model, where SBL experiments depend on the seven parameters listed in Table II. In addition to the two mass-squared differences and the moduli of the mixing matrix elements, also a physical complex phase enters, $\delta \equiv \arg(U_{\mu 4} U^*_{e4} U^*_{\mu 5} U_{e5})$. This phase leads to *CP* violation in SBL oscillations [8,24], allowing the reconciliation of differing neutrino and antineutrino results from MiniBooNE/LSND. Table II shows the parameter

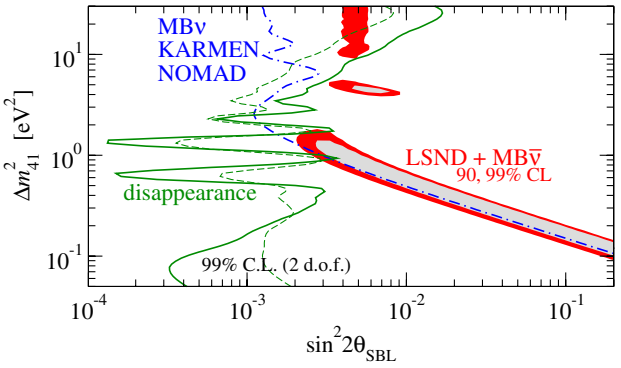

FIG. 3 (color online). Global constraints on sterile neutrinos in the 3 + 1 model. We show the allowed regions at 90% and 99% C.L. from a combined analysis of the LSND [3] and MiniBooNE antineutrino [4] signals (filled regions), as well as the constraints from the null results of KARMEN [20], NOMAD [21] and MiniBooNE neutrino [19] appearance searches (blue dot-dashed contour). The limit from disappearance experiments includes data from CDHS [22], atmospheric neutrinos, and from the SBL reactor experiments. We compare results obtained using the new $\bar{\nu}_e$ flux prediction [5] (solid) to those obtained using the previous prediction [6] (dashed). The region to the right of the curves is excluded at 99% C.L.

TABLE II. Parameter values and χ^2 at the global best-fit points for 3 + 2 and 1 + 3 + 1 oscillations (Δm^2's in eV^2).

	Δm^2_{41}	$\lvert U_{e4}\rvert$	$\lvert U_{\mu 4}\rvert$	Δm^2_{51}	$\lvert U_{e5}\rvert$	$\lvert U_{\mu 5}\rvert$	δ/π	χ^2/d.o.f.
3 + 2	0.47	0.128	0.165	0.87	0.138	0.148	1.64	110.1/130
1 + 3 + 1	0.47	0.129	0.154	0.87	0.142	0.163	0.35	106.1/130

values at the global best-fit point and the corresponding χ^2 value. Changing from the previous to the new reactor flux calculations the χ^2 decreases by 10.6 units, indicating a significant improvement of the description of the data; see also upper panel of Fig. 2. From that figure follows also that going from 3 + 1 to 3 + 2 leads to a significant improvement of the fit with the new reactor fluxes, which was not the case with the old ones. The χ^2 improves by 11.2 units, which means that 3 + 1 is disfavored at the 97.6% C.L. (4 d.o.f.) with respect to 3 + 2, compared to $\Delta\chi^2 = 6.3$ (82% C.L.) for old fluxes.

In Fig. 1 we show the prediction for the Bugey spectra at the global best-fit point as dashed curves. Clearly they are very similar to the best fit of reactor data only. Figure 4 shows the predicted spectra for MiniBooNE neutrino and antineutrino data, as well as the LSND $\bar{\nu}_\mu \to \bar{\nu}_e$ transition probability. Again we find an acceptable fit to the data, although in this case the fit is slightly worse than a fit to appearance data only (dashed histograms). Note that MiniBooNE observes an event excess in the lower part of the spectrum. This excess can be explained if only appearance data are considered, but not in the global analysis including disappearance searches [8]. Therefore, we follow [19] and assume an alternative explanation for this excess, e.g., [25]. In Table III we show the compatibility of the LSND/MiniBooNE($\bar{\nu}$) signal with the rest of the data, as well as the compatibility of appearance and disappearance searches using the PG test from [23]. Although the compatibility improves drastically when changing from old to new reactor fluxes, the PG is still below 1% for 3 + 2. This indicates that some tension between data sets remains. We considered also a "1 + 3 + 1" scenario, in which one of

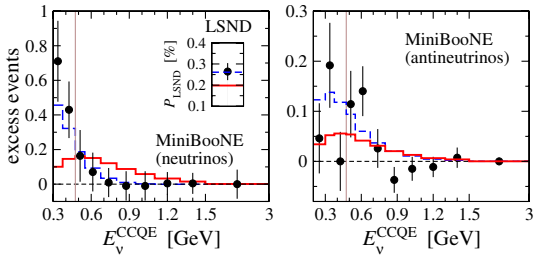

FIG. 4 (color online). Predicted spectra for MiniBooNE data and the transition probability for LSND (inset). Solid histograms refer to the 3 + 2 global best-fit point (Table II), dashed histograms correspond to the best fit of appearance data only (LSND, MiniBooNE $\nu/\bar{\nu}$, KARMEN, NOMAD). For MiniBooNE we fit only data above 475 MeV.

TABLE III. Compatibility of data sets [23] for 3 + 2 and 1 + 3 + 1 oscillations using old and new reactor fluxes.

	LSND + MB($\bar{\nu}$) vs rest		Appearance vs disappearance	
	Old	New	Old	New
$\chi^2_{\mathrm{PG},3+2}$/d.o.f.	25.1/5	19.9/5	19.9/4	14.7/4
PG_{3+2}	10^{-4}	0.13%	5×10^{-4}	0.53%
$\chi^2_{\mathrm{PG},1+3+1}$/d.o.f.	19.6/5	16.0/5	14.4/4	10.6/4
PG_{1+3+1}	0.14%	0.7%	0.6%	3%

the sterile mass eigenstates is lighter than the three active ones and the other is heavier [26]. As can be seen from Tables II and III the fit of 1 + 3 + 1 is slightly better than 3 + 2, with $\Delta\chi^2 = 15.2$ between 3 + 1 and 1 + 3 + 1 (99.6% C.L. for 4 d.o.f.). However, due to the larger total mass in neutrinos, a 1 + 3 + 1 ordering might be in more tension with cosmology than a 3 + 2 scheme [27–29]. Figure 5 shows the allowed regions for the two mass-squared differences for the 3 + 2 and 1 + 3 + 1 schemes.

Discussion.—Let us comment briefly on other signatures of eV-scale sterile neutrinos. We have checked the fit of solar neutrino data and the KamLAND reactor experiment, and found excellent agreement. The effect of nonzero U_{e4} and U_{e5} for these data is similar to the one of U_{e3} in the standard three-active neutrino case, and hence the 3 + 2 best-fit point mimics a nonzero U_{e3} close to the preferred value of these data; see [1,2,30]. Our best-fit points also fall in the range of parameter values required to explain the small ν_e deficit observed in radioactive source measurements at radiochemical neutrino detectors [31]. The MINOS long-baseline experiment has performed a search for sterile neutrinos via neutral current (NC) measurements [32]. We have estimated that the best-fit points reported in Table II lead to an increase of the χ^2 of MINOS NC data as well as χ^2_{PG} by a few units [30]. Finally, sterile neutrinos may manifest themselves in cosmology. Recent studies [27–29] indicate a slight preference for extra radiation content in the Universe (mainly from CMB measurements), favoring the existence of light sterile neutrinos. On the other hand, big-bang nucleosynthesis constrains the number of extra neutrino species to be <1.2 at 95% C.L. [33], which may be a challenge for two sterile neutrino schemes. Moreover, global fits to cosmological data constrain the sum of the neutrino masses to be ≤ 0.7 to 1.5 eV at 95% C.L. [27–29], depending on the used data, whereas our 3 + 2 best-fit point leads to $\sum m_\nu \approx 1.7$ eV. Hence, sterile neutrino explanations of short-baseline oscillation data are in tension with cosmology, or, if confirmed, would indicate a deviation from the standard cosmological picture.

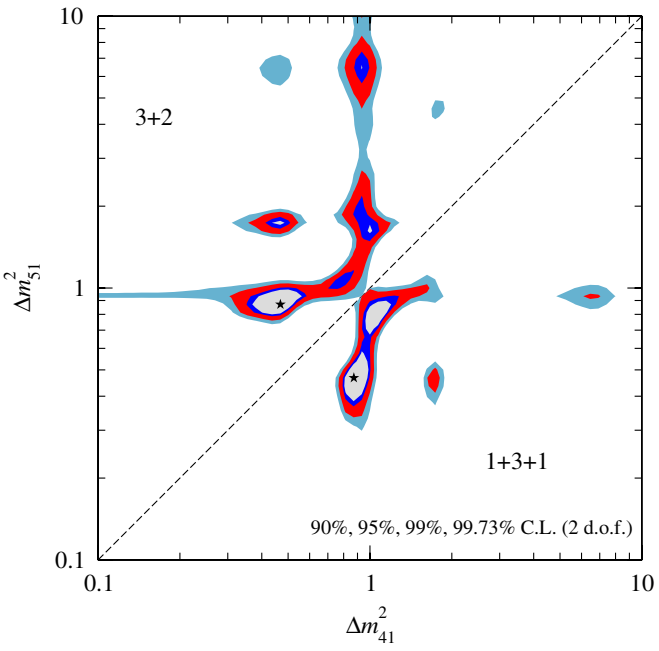

FIG. 5 (color online). The globally preferred regions for the neutrino mass-squared differences Δm^2_{41} and Δm^2_{51} in the 3 + 2 (upper left) and 1 + 3 + 1 (lower right) scenarios.

In conclusion, we have shown that a global fit to short-baseline oscillation searches assuming two sterile neutrinos improves significantly when new predictions for the reactor neutrino flux are taken into account, although some tension remains. We are thus facing an intriguing accumulation of hints for the existence of sterile neutrinos at the eV scale, and a confirmation of these hints in the future would certainly be considered a major discovery.

This work was supported by the U.S. Department of Energy (DE-AC02-07CH11359), the Spanish MICINN (FPA-2009-08958, FPA-2009-09017, CSD-2008-0037), the Comunidad Autnoma de Madrid (HEPHACOS S2009/ESP-1473), the Deutsche Forschungsgemeinschaft, and the European Union (EUROν).

[1] T. Schwetz, M. Tortola, and J. W. F. Valle, New J. Phys. **13**, 063004 (2011).
[2] M. C. Gonzalez-Garcia *et al.*, J. High Energy Phys. 04 (2010) 056.
[3] A. Aguilar *et al.*, Phys. Rev. D **64**, 112007 (2001).
[4] A. A. Aguilar *et al.*, Phys. Rev. Lett. **105**, 181801 (2010).
[5] T. A. Mueller *et al.*, Phys. Rev. C **83**, 054615 (2011).
[6] K. Schreckenbach *et al.*, Phys. Lett. B **160**, 325 (1985).
[7] G. Mention *et al.*, Phys. Rev. D **83**, 073006 (2011).

[8] M. Maltoni and T. Schwetz, Phys. Rev. D **76**, 093005 (2007).
[9] G. Karagiorgi *et al.*, Phys. Rev. D **80**, 073001 (2009).
[10] E. Akhmedov and T. Schwetz, J. High Energy Phys. 10 (2010) 115.
[11] Y. Declais *et al.*, Nucl. Phys. **B434**, 503 (1995).
[12] Y. Declais *et al.*, Phys. Lett. B **338**, 383 (1994).
[13] A. Kuvshinnikov *et al.*, JETP Lett. **54**, 253 (1991).
[14] G. Vidyakin *et al.*, Sov. Phys. JETP **66**, 243 (1987).
[15] H. Kwon *et al.*, Phys. Rev. D **24**, 1097 (1981).
[16] G. Zacek *et al.*, Phys. Rev. D **34**, 2621 (1986).
[17] M. Apollonio *et al.*, Eur. Phys. J. C **27**, 331 (2003).
[18] F. Boehm *et al.*, Phys. Rev. D **64**, 112001 (2001).
[19] A. Aguilar *et al.*, Phys. Rev. Lett. **98**, 231801 (2007).
[20] B. Armbruster *et al.*, Phys. Rev. D **65**, 112001 (2002).
[21] P. Astier *et al.*, Nucl. Phys. **B611**, 3 (2001).
[22] F. Dydak *et al.*, Phys. Lett. B **134**, 281 (1984).
[23] M. Maltoni and T. Schwetz, Phys. Rev. D **68**, 033020 (2003).
[24] G. Karagiorgi *et al.*, Phys. Rev. D **75**, 013011 (2007).
[25] R. J. Hill, Phys. Rev. D **84**, 017501 (2011).
[26] S. Goswami and W. Rodejohann, J. High Energy Phys. 10 (2007) 073.
[27] M. C. Gonzalez-Garcia *et al.*, J. High Energy Phys. 08 (2010) 117.
[28] J. Hamann *et al.*, Phys. Rev. Lett. **105**, 181301 (2010).
[29] E. Giusarma *et al.*, Phys. Rev. D **83**, 115023 (2011).
[30] J. Kopp, M. Maltoni, and T. Schwetz (to be published).
[31] M. A. Acero *et al.*, Phys. Rev. D **78**, 073009 (2008).
[32] P. Adamson *et al.*, Phys. Rev. D **81**, 052004 (2010).
[33] G. Mangano and P. D. Serpico, Phys. Lett. B **701**, 296 (2011).